

42. MAGNETIC PROPERTIES AND DOMAIN STATE OF BASALT CORES FROM THE NAZCA PLATE

E.R. Deutsch and R.R. Pätzold, Geomagnetic Research Laboratory, Physics Department, Memorial University of Newfoundland, St. John's, Canada

INTRODUCTION

In this paper we present results of magnetic studies on 46 minicore basalt samples from the three sites (319, 320, 321) of Deep-Sea Drilling Project Leg 34. For background, the reader is referred to papers on the Nazca plate (e.g., Herron, 1972) and to other chapters in this volume. Our twofold objective was (1) to obtain clues from paleomagnetic measurements on possible horizontal displacements of the Nazca plate, and (2) to infer magnetic stability, domain state and magnetic composition from determinations of some magnetic properties and their temperature dependence. Paleomagnetic interpretations are limited by the fact that the cores lack an azimuthal orientation, allowing inclination (I) but not the total remanence vector to be measured. Therefore, in this work we have placed more emphasis on objective (2) than on (1). Knowledge of the ferromagnetic structure of these rocks should throw light on the nature of the magnetized layer and to enable one to formulate realistic models for magnetic anomaly interpretation. Towards that end we have made use of the magnetic granulometry technique for basalts developed at the Tata Institute of Fundamental Research, Bombay (Radhakrishnamurty and Likhite, 1970; Radhakrishnamurty and Deutsch, 1974), employing hysteresis and susceptibility measurements as a function of temperature for distinguishing multidomain (MD), singledomain (SD), and superparamagnetic (SP) content in the magnetite-maghemite compositional range. These tests have the advantage of relative speed over other diagnostic procedures (e.g., Dunlop, 1965; Lowrie and Fuller, 1971).

EXPERIMENTAL PROCEDURE

The prospect of not being able to resample called for special care in planning measurements. Three types of magnetic measurements were carried out:

A) Nondestructive tests—the direction and intensity of the natural remanence (NRM), initial susceptibility (k), and low-field hysteresis were measured on all 46 samples.

B) Semidestructive tests—comprising alternating-field (AF) demagnetization and high-field hysteresis.

C) Destructive tests—comprising thermal demagnetization, acquisition of thermoremanence (TRM), and measurement of susceptibility and magnetic moment (M) versus temperature.

Table 1 and its footnotes elaborate on the experimental scheme applied to different sets and subsets of the samples. To further study irreversible effects caused by heat treatments, some hysteresis measurements on samples that had been heated were repeated.

The following apparatus was used, at fields and temperatures given in footnotes to Table 1:

1) PAR spinner magnetometer to measure room-temperature remanence. Single measurements were usually repeatable to 1% in intensity and 1° in direction.

2, 3) Rayleigh loop tracer and high-field hysteresis loop tracer (Likhite et al., 1965), both for display of these loops on an oscilloscope. At -196°C , high-field loops were obtained upon withdrawal of samples from a liquid nitrogen bath.

4) AF demagnetizing unit with 3-axis tumbler.

5) Furnace for stepwise thermal demagnetization, using standard procedures.

6) Astatic magnetometer for measuring continuous thermal decay of remanence by Wilson's (1962) method. The advantage over the more rapid stepwise technique is that all measurements are made at the effective temperature during one heating cycle. Our recently built instrument incorporates transversely magnetized Magnadur III magnets of high magnetic moment/moment of inertia ratio and a water-cooled furnace designed at the Tata Institute of Fundamental Research, Bombay.

7) Low-field ac susceptibility (k) bridge of Christie and Symons (1969) type, adapted for measurement of k versus temperature by Pätzold (1972), in the range -196° to 20°C , k - T curves are recorded during natural heating of samples after immersion in liquid nitrogen. Between 20° - 650°C both heating and cooling curves are traced, using a water-cooled furnace. After cooling, the cycle is completed by repeating the -196°C to 20°C measurement, so that each "cooling" curve actually consists of a cooling and a heating section, meeting at 20°C . The two sections always coincided at 20°C , indicating that, in the interval -196°C to 20°C , k was reversible. For our samples the range of expected errors in k is 2.5%-5% at low to room temperatures and 4%-10% at high temperatures.

8) Vertical balance (Deutsch et al., 1971) for measuring high-field magnetic moment versus temperature (M - T curves), giving Curie points (T_c) to $\pm 15^\circ\text{C}$ or less, repeatable to $\pm 5^\circ\text{C}$.

All measurements were in air. Instruments (1) and (4-7) were operated in cancelled fields. In the stepwise thermal unit (5), residual fields were at most 50γ , but usually less. All furnaces are noninductive. Estimated errors in T above 20°C are $\pm 10^\circ\text{C}$ or less, but may be $> 10\%$ in the -196° to 20°C range of the k - T curves, where there is no control of heating rate.

NONDESTRUCTIVE MEASUREMENTS

Most of our samples came from Sites 319 (27 samples) and 321 (17 samples). At these locations the quoted age

TABLE 1
Experimental Scheme

No.	Sample (Interval in cm)	Demagnetization			High-Field Hysteresis		M-T
		AF	Thermal		Treated	Fresh	
			Step.	Cont.			
Hole 319							
1	13-1, 138-141				5		
2	13-1, 144-147				6b	6a	7
Hole 319A							
3	1-1, 23-26				5		
4	1-1, 42-45	1					
5	2-2, 87-90				5		
6	2-3, 75-78				6	7	7a
7	3-1, 50-53				4		
8	3-1, 89-92	1					
9	3-2, 9-12		2				
10	3-2, 70-73	1					
11	3-2, 104-107			3		3a	
12	3-3, 14-17	1					
13	3-3, 64-67				4		
14	3-3, 110-113	1					
15	3-3, 119-122		2				
16	3-4, 37-40	1					
17	3-4, 96-99			3	3b	3a	
18	3-4, 136-139				6	7	7a
19	3-5, 44-47		2				
20	3-5, 73-75	1					
21	3-5, 78-81				6	6b	7
22	4-1, 119-122			3	3b	6a	7
23	4-1, 123-126				6	7	7a
24	5-1, 68-71			3		3a	
25	5-1, 84-87				6	7	7a
26	7-1, 68-71			3	3b	3a	
27	7-1, 96-99				6		7
Hole 320B							
28	3-1, 73-76				6		7
29	3-1, 136-139		2				7a
Site 321							
30	14-1, 52-55	1					
31	14-1, 55-58	1					
32	14-1, 88-91				4		
33	14-1, 99-102		2				
34	14-1, 142-145			3	3b	3a	
35	14-2, 49-51	1					
36	14-2, 50-53				6	6b	7
37	14-2, 94-97	1					7a
38	14-2, 122-125			3		3a	
39	14-3, 1-4	1					
40	14-3, 4-7				4		
41	14-3, 97-100	1					
42	14-3, 103-106		2				
43	14-4, 12-15	1					
44	14-4, 35-38			3	3b	3a	
45	14-4, 42-45	1					
46	14-4, 64-67			3	3b	3a	

NOTE: The following parameters were obtained from nondestructive tests on all 46 samples prior to experiments listed in this table (AF values quoted in peak oersted): (i) Direction and intensity (J_n , G) of natural remanence (NRM); (ii) Initial susceptibility (k , G/oe, measured in 0.31 oe); (iii) Koenigsberger ratio ($Q_n = J_n/kH$, where $H = 0.30$ oe is the present in-situ field); (iv) Hysteresis (Rayleigh loops) measured in 10 oe. In columns starting with "AF," numbers 1 to 7 not followed by letters each refer to a set of whole samples (No. 1-5) or half samples (No. 6, 7) that were fresh, except for nondestructive tests. Each case in Set 6 represents one half and Set 7 the other half of one original sample, bisected so that two parallel destructive tests could be made and also because the high-field hysteresis unit accommodates only half samples. Small letters after numbers denote subsequent treatments in the order a, b. Thus 6, 6a, 6b (or 7, 7a) is a sequence of experiments performed on the same originally fresh half sample; in the case of tests 3a, 3b, a half sample cut from the Set 3 (whole) sample after thermal treatment was used. Experiments performed on fresh rock: Set 1 - Alternating-field demagnetization using fields of 25, 50, 100, 150, 200, 250, 300, 400, 600, and 850 (oe). Set 2 - Stepwise thermal demagnetization using temperatures of 50, 75, 100, 150, 250, 300, 350, 400, 500, 550, 600, and 700 (°C). Set 3 - Continuous thermal demagnetization to 625°C. The remanence was measured during the heating cycle at 50, 100, 150, 200, 250, 300, 400, 500, 550, and 600 (°C). Set 4 - Continuous susceptibility-temperature (k -T) measurements between -196° and 650°C in a field of 0.31 oe. Set 5 - $Q_t = J_t/k_tH$, where J_t is the thermoremanence (TRM) and k_t is susceptibility measured at 20°C after heating the rock to > 600°C and cooling in a field $H = 0.30$ oe equal to the in situ field. Set 6 - As Set 4, but using half samples. Set 7 - High-field hysteresis measurement in 1200 oe at -196° and 20°C. Experiments performed on treated rock: Subset 3a - Rayleigh loops followed by high-field hysteresis (as Set 7). Subset 3b - Q_t (as Set 5). Subset 6a - High-field hysteresis (as Set 7). Subset 6b - Q_t (as Set 5). Subset 7a - Magnetic moment-temperature (M-T) measured to 625°C in 1300 oe on powder derived from half samples used previously in Set 7.

of the basement is 15 m.y. and 40 m.y., respectively. Hart et al. (1974) have compared these rocks as follows: The 59 meters of interlayered pillow lavas and massive flows penetrated at Site 319 are among the freshest basalts yet sampled during the Deep Sea Drilling Project and the 11-meter basalt column drilled at Site 321, comprising massive flows, is very similar in its mineralogy, physical properties, and low degree of alteration to the Site 319 flows. The fine-grained basalt penetrated at Site 320 is more altered but still relatively fresh for basement rock of this age (28 m.y.). Petrographic analysis by Ade-Hall et al. (Petrography of Opaque Minerals, this volume) showed that magnetite associated with titanium is everywhere the dominant opaque phase in Leg 34 basalts.

The following ranges of values of NRM intensity, susceptibility, and Koenigsberger ratio were obtained by us (hole numbers in italics):

J_n ($G \times 10^{-3}$): 319 (2 samples), 1.4 and 1.9; 319A (25 samples), 0.22 to 3.2; 320B (2 samples), 0.10 and 0.48; 321 (17 samples), 4.2 to 17.

k ($G \text{ oe} \times 10^{-3}$): 319, 0.58 and 0.90; 319A, 0.11 to 3.3; 320B, 0.12 and 0.16; 321, 0.28 to 4.8.

Q_n : 319, 7.1 and 7.8; 319A, 0.28 to 30; 320B, 2.0 and 13; 321, 3.4 to 157.

Averages of these three parameters for Hole 319A and Site 321 are given in Table 2 (third and fourth rows). All six mean values fall within the range of J_n , k , or Q_n values cited by Lowrie (1974) for basalts from 26 previous DSDP sites, including six sites in the Pacific Ocean. His overall \bar{J}_n and \bar{Q}_n averages (Table 2) fall between our respective values for Hole 319A and Site 321; this applies even if \bar{J}_n and \bar{Q}_n for Hole 319A were to be raised some 40% to correct for an upward-directed soft component acquired through drilling (Ade-Hall and Johnson, Review of Magnetic Properties, this volume). However, Lowrie's k value is lower than k for either 319A or 321. Dredged basalts (Table 2) often exhibit still lower susceptibility along with large NRM intensity and large Koenigsberger ratios, indicating that induced components are unimportant. However, about half the drill sites in Lowrie's tabulation have Q_n values less than 10, as is the case also in almost three-quarters of our samples, including six samples from Hole 319A where $Q_n \leq 1$. Thus the assumption of a negligible induced component usually made in interpreting sea-floor magnetic anomalies in the context of the Vine-Matthews hypothesis does not necessarily apply to the basalt of Leg 34.

It is interesting that the \bar{J}_n , \bar{k} , and \bar{Q}_n values for Site 321 all exceed those for Hole 319A— J_n by a factor of nine—despite the reported physical-chemical similarities between the basalts at the two sites. Among possible causes we suspected that between-site differences in the domain state and perhaps also in the oxidation state of the magnetite might be crucial. An initial test, for low-field hysteresis, showed that 14 out of 25 samples from Hole 319A and all 17 samples from Site 321 exhibit Rayleigh loops in 10 oe, while the remaining 11 samples from Hole 319A and the two samples each from Holes 319 and 320B did not exhibit loops. Examples of these two kinds of behavior, shown in Figure 1a, b, are denoted "Type I" and "Type II," respectively, by

association of low-field hysteresis with k - T curves to be discussed later. Separate averaging for the two kinds of samples from Hole 319A (Table 2) reveals striking disparities: the susceptibility of the set showing Rayleigh loops is 11 times as large and its Koenigsberger ratio is less than one-sixth as large as in the set showing no loops.

Radhakrishnamurty and Likhite (1970) attribute the appearance of Rayleigh loops in basalts at room temperature to the presence of very fine singledomain particles, a significant fraction of which are superparamagnetic. In a given material the susceptibility contributed by an SP fraction can be much greater than that due to the same concentration of larger grains (Bean and Livingstone, 1959). In this way one could account for the relatively large \bar{k} and small \bar{Q}_n of the Hole 319A samples showing Rayleigh loops. It is more difficult to explain why these samples have a larger \bar{J}_n than do the samples showing no loops or why the \bar{J}_n value for Site 321 is so large, whereas ideally a cluster of SP grains should have no remanence. However, natural SP assemblies, such as in rocks, probably always show some dipole interaction and also one would normally expect the magnetic particle size distribution of a rock containing SP to extend into the stable singledomain region of the spectrum. Thus, depending on the contributions from SP interaction and SD content, a rock exhibiting some superparamagnetism might have an appreciable remanence.

We should point out that, for the reasons just given and for convenience, the designation "SP" is being used somewhat loosely in this chapter. For example, later we invoke the presence of "SP particles" to explain the observed properties at 20°C of samples whose mean blocking temperature might be 100°C or less. Assuming the particles are indeed single domains, it is probably more accurate to describe the dominant fraction as "very fine particles just above SP/SD threshold size," though in most cases such a sample would almost certainly also contain still finer material having true SP character at 20°C. Thus, when speaking of "SP particles" or an "SP fraction" we imply the actual presence of some size *distribution*, as above.

A further clue to the cause of large J_n values in samples showing Rayleigh loops may be the fact that, in

9 out of 17 samples from Site 321, but in only one marginal case (Sample 4) from Hole 319A, the loops were constricted (Figure 2). Radhakrishnamurty and Sastry (1970) and Néel (1970) have attributed such constrictions to strong interaction in dense SP particle clusters. This should correspond to an intermediate case between SD and SP where one might expect both the remanence and the susceptibility to be large, as is indeed the case at Site 321. In the absence of further data, the above explanation must remain somewhat speculative.

PALEOMAGNETISM

Fifteen samples from Hole 319A and 14 from Site 321 were subjected to AF and thermal demagnetization in an attempt to isolate a stable component from which the site mean inclinations could be calculated.

Hole 319A

All inclination values for Hole 319A are subject to an error of $\pm 3^\circ$ or less, due to a 3° departure of the drill axis from the vertical. Figure 3 shows the response to AF demagnetization of one sample each of Types I and II. Sample 20 (Type I) lost most of its NRM in fields less than 100 oe. This loss and the intensity peak at 25 oe (Figure 3a) both can be explained by the removal of a prominent negative viscous (VRM) component superimposed on a more stable positive component. Figure 3b shows the corresponding directional changes, using an arbitrary reference for declinations. The remanence directions became stabilized in the range 25-200 oe, but moved through large angles in higher fields. Sample 12 (Type II) was less easily demagnetized, the median destructive field $H_{1/2}$ being about 150 oe (Figure 3c). In this case the NRM direction remained quite stable in fields up to 250 oe, but even larger angular shifts than in Sample 20 occurred at higher fields (Figure 3d).

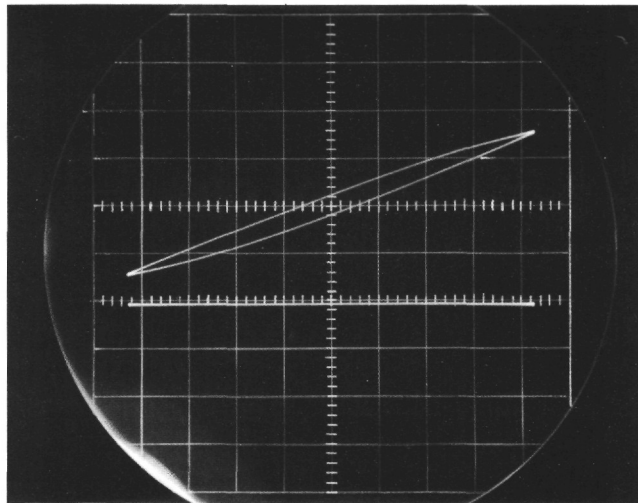
Results for continuous thermal demagnetization are shown in Figure 4. The behavior of Sample 22 (Type I) is similar to that of Sample 20, above; removal of a prominent negative VRM superimposed on a more stable positive component can explain both the large intensity loss and the change from steeply negative to steeply positive directions between NRM and 100°C. Again the directions became stabilized in an in-

TABLE 2
Summarized Results of Nondestructive Tests

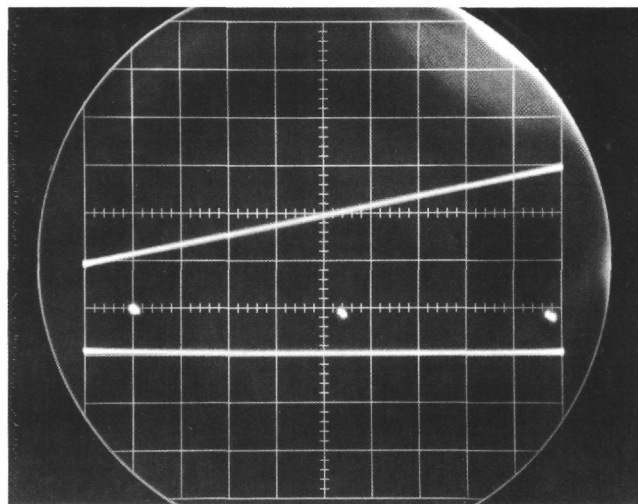
Hole	Rayleigh Loops	N	\bar{J}_n (10^{-3} G)	\bar{k} (10^{-3} G/oe)	\bar{Q}_n
319A	No	11	0.768	0.242	10.1
319A	Yes	14	1.32	0.265	1.6
319A	Combined	25	1.04	0.924	3.6
321	Yes	17	9.34	2.30	12.9
DSDP sites ^a	—	26	2.06	0.632	7.92
Dredge sites ^a	—	110	5.76	0.318	39.9

NOTE: J_n = Intensity of the NRM; k = Initial susceptibility; Q_n = Koenigsberger ratio $- J_n/kH$, where H is the present mean in situ field; \bar{J}_n , \bar{k} , and \bar{Q}_n are geometric mean values for N samples or sites (italicized numbers).

^aPublished data for basalts from various oceans cited by Lowrie (1974).



(a)



(b)

Figure 1. Photographs of open and closed Rayleigh loops with horizontal reference traces in 10-oe peak corresponding to (a) Type I, Sample 24; (b) Type II, Sample 11. The vertical (J) scale is arbitrary.

intermediate range (100°-300°C), followed by large-angle changes on further heating. Once more Type II (Sample 26), with median destructive temperature $T_{1/2} \approx 250^\circ\text{C}$, showed greater stability than Type I ($T_{1/2} < 50^\circ\text{C}$), and the NRM of the former was directionally very stable up to 250°C.

Figures 3 and 4 are in general representative examples also of the Type I or II behavior of the 11 additional thermally and AF-demagnetized samples (not included in figures). Also, no systematic differences between the results of continuous and stepwise thermal treatment were found. In our interpretation, the low coercivity VRM prominent especially in Type I samples appears to

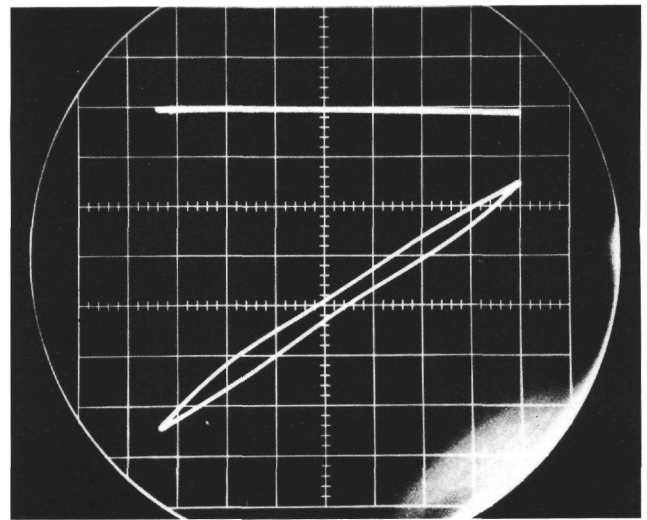


Figure 2. Photograph of constricted Rayleigh loop, Sample 30. Notation as in Figure 1. Note positioning error with respect to origin.

be due to the presence of an SP fraction, while the directional stability observed in samples of both types at low to intermediate fields or temperatures may be attributed to a moderately stable SD fraction.

Since the remanence directions became unstable at higher fields and temperatures, the method of stable end-points often used in estimating optimum demagnetization steps cannot be applied here. The method of tightest vector grouping of samples is also inapplicable, since declinations are not known. One could use as a criterion the least didirectional change (γ_{\min}) occurring between any two demagnetization steps for a sample. Table 3 (first two lines) shows for the N samples in each set the field or temperature range over which γ_{\min} values occurred. These ranges correspond to the curve segments showing small vector displacements in Figures 3b, d and 4b, d. Observed γ_{\min} values for AF or thermal demagnetization were 1° to 11°, although much larger directional changes were common at off-optimum fields and temperatures. However, the treatment steps at which γ became minimum varied from sample to sample. Therefore, the mean inclination (\bar{I}) finally was estimated by choosing that field or temperature step giving the smallest standard deviation (σ) in \bar{I} . These steps fall within the respective ranges of γ_{\min} for Hole 319A (Table 3). The implied assumption in regarding the least- σ step as optimum is that at or close to the same step Fisher statistics would yield the smallest circle of confidence if absolute directions were known, which seems reasonable.

Sample 16 showed discordant negative inclinations throughout AF treatment and was excluded from the set. The other six samples and the eight thermally treated samples gave $\bar{I} = +46^\circ \pm 9^\circ$ and $\bar{I} = +58^\circ \pm 8^\circ$, respectively, with a combined value $\bar{I} = +53^\circ$. This is close to the values (+53° to +58°) quoted by three other research groups (Ade-Hall and Johnson, Review of Magnetic Properties, this volume). At Site 319 (latitude 13°S) the field inclination for an axial dipole of normal

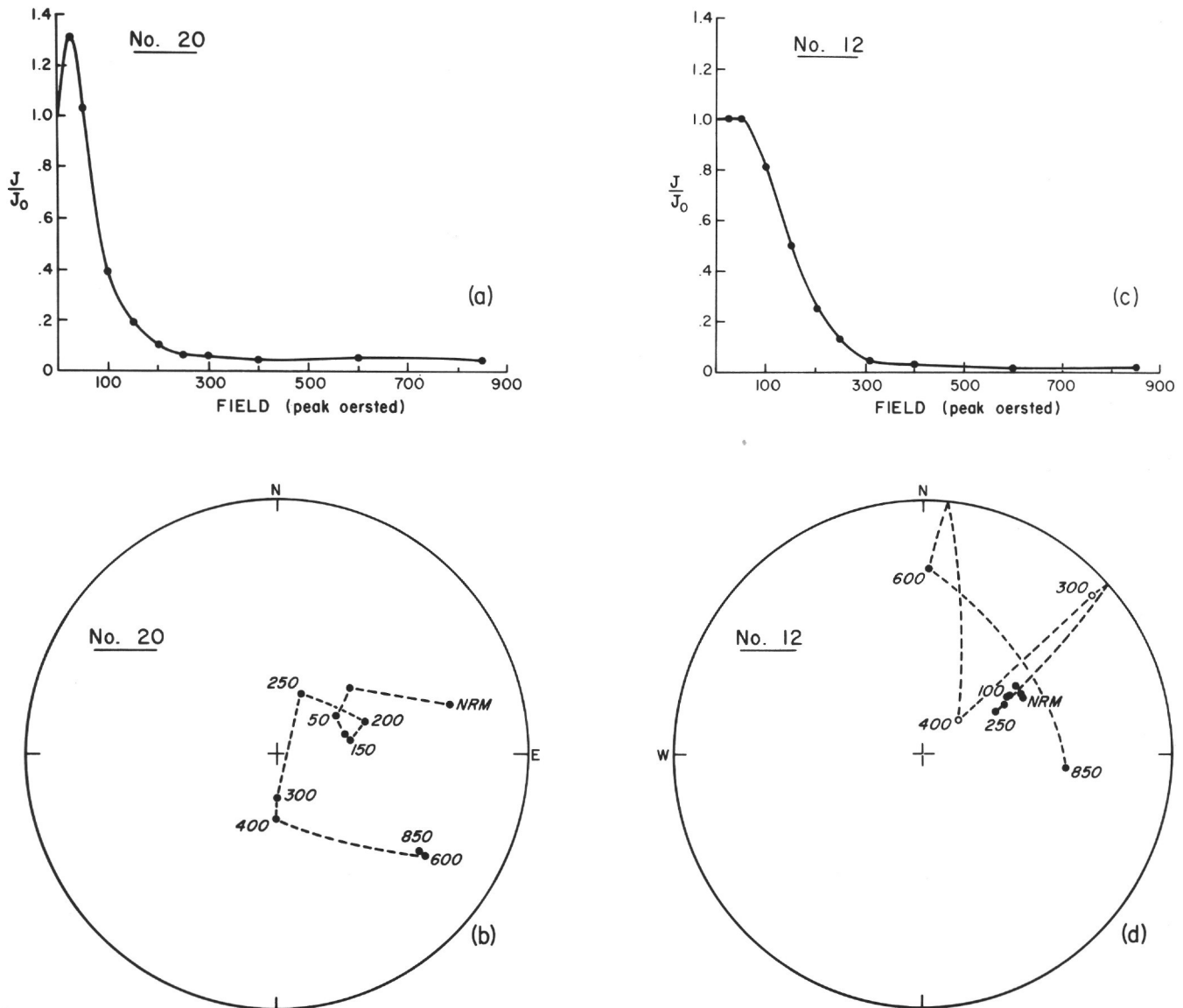


Figure 3. (a, c) Normalized remanence versus temperature in continuous thermal demagnetization; and (b, d) Corresponding directional changes plotted on a stereographic (Wulff's) projection with the circumference as horizontal. Open and closed dots represent positive (north pole downward) and negative directions, respectively. (a, b) Type I; (c, d) Type II.

polarity is -25° . Possible explanations for this large discrepancy, discussed by Ade-Hall and Johnson, include (a) unrepresentative sampling of the geomagnetic field; (b) local tectonic tilting; and (c) large latitudinal motions of the Nazca plate, either wouthward assuming the basalts have normal polarity, or northward assuming reverse polarity. However, a serious objection against alternative (c) pointed out by these authors is that, in contrast with the above result, the inclinations of the basalt at Sites 321 (see below) and 320, as well as those of the sediments overlying the basalt at Site 319 (Ade-Hall and Johnson, this volume), have low negative values close to dipole field directions at these sites. Paleomagnetic interpretations will not be attempted here.

Site 321

As all our samples from Site 321 showed Rayleigh loops, their behavior on demagnetization was expected

to be of Type I (compare Figures 3a, b and 4a, b). This was generally the case, though in two or three of the thermal decay curves (not shown) the trend was intermediate between Types I and II. The mean inclination for AF treatment at 150 oe is $-17^\circ \pm 5^\circ$ and that for thermal treatment at 50°C is $-13^\circ \pm 3^\circ$ (Table 3). Note that 50°C lies below the range of γ_{min} for the six thermally treated samples. The combined value for the 14 samples is $\bar{I} = -15^\circ$, which is reasonably close both to the axial dipole value for Site 321 ($I = -25^\circ$) and to the inclinations (-16° to -24°), quoted by three other research groups (Ade-Hall and Johnson, Review of Magnetic Properties, this volume). Table 3 shows that the difference between \bar{I} values obtained from AF and thermal treatment as well as both standard deviation values are less for Site 321 than for Hole 319A. It does not follow, however, that the magnetization of the basalts from Site 321 is more stable: rather, the relative agreement found between the stable remanence inclina-

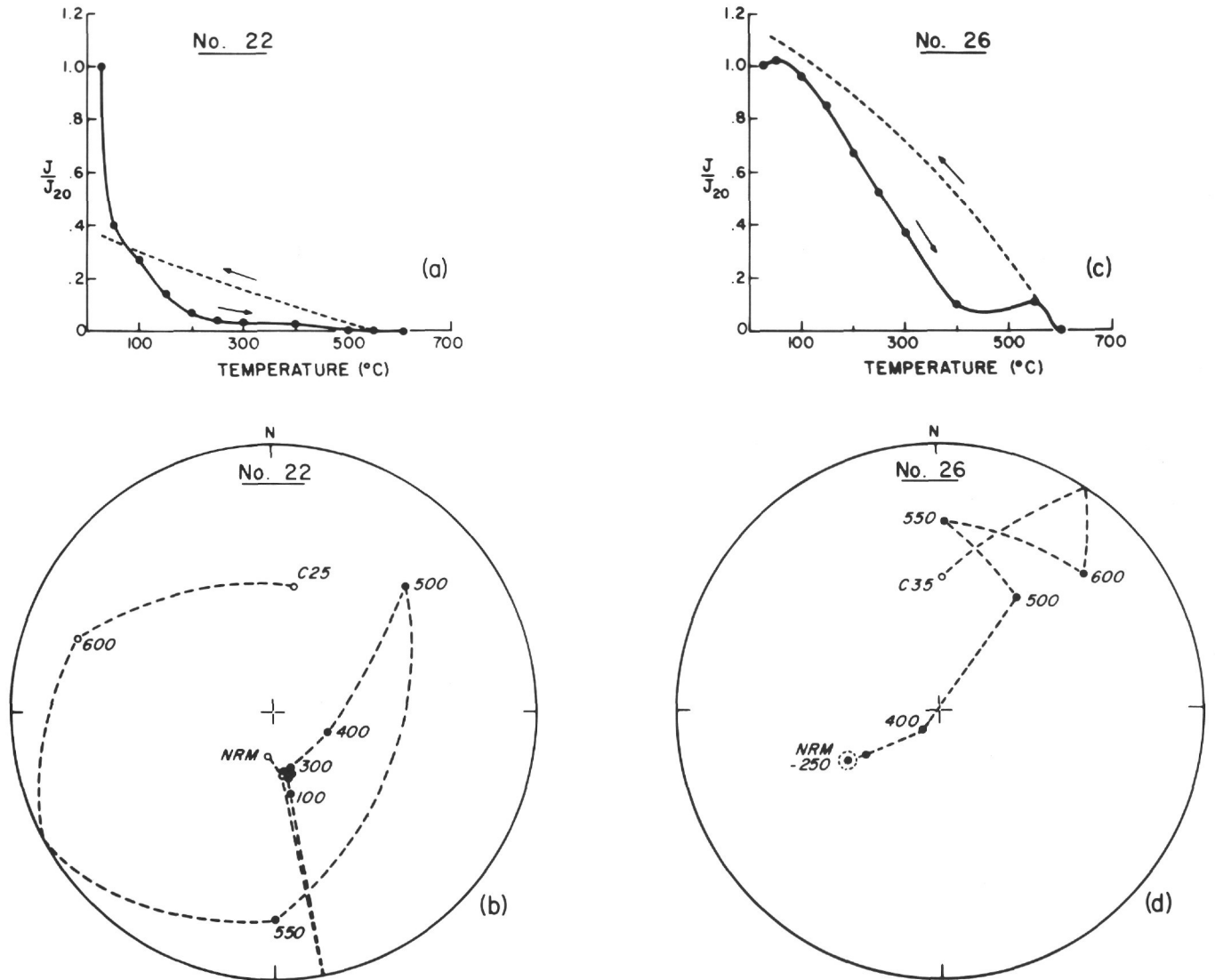


Figure 4. (a, c) Normalized remanence versus temperature in continuous thermal demagnetization; and (b, d) Corresponding directional changes plotted on a Wulff net. Directions measured after cooling are denoted C25 and C35 (°C); other notations are as in Figure 3. (a, b) Type I; (c, d) Type II.

TABLE 3
Mean Inclination of the Stable Component

Hole/ Site	Treatment	N	Range of γ_{\min}	Treatment Step for Least σ	Best \bar{I}
319A	AF	6	100-250 oe	200 oe	+46° ± 9°
319A	Thermal	8	100-300 °C	250 °C	+58° ± 8°
321	AF	8	50-250 oe	150 oe	-17° ± 5°
321	Thermal	6	100-250 °C	50 °C	-13° ± 3°
319A	Combined	14	-	-	+53°
321	Combined	14	-	-	-15°

NOTE: For any sample, γ (degrees of arc) is the change in remanence direction between any two steps in the treatment; γ_{\min} is the least γ value during the treatment. For the N samples, γ_{\min} lies in the range shown; σ = Standard deviation of mean inclination \bar{I} (positive downwards), for a given step in the treatment; Best \bar{I} = mean inclination and σ , for step shown in previous column; AF = Alternating-field demagnetization; Thermal combines treatments by stepwise and continuous techniques.

tion and the field inclination, in contrast with Hole 319A, should lead one to expect that samples from Site 321 will show close alignment between the stable component and any VRM that is not so unstable as to be strongly affected by laboratory fields.

MAGNETIC PROPERTIES

We shall now summarize the results of some other magnetic experiments and discuss these in the context of contrasting properties previously denoted Type I and Type II. Since both types of behavior, in terms of low-field hysteresis, were found in samples from Site 319, all examples shown in Figures 3-7 are based on that site.

Low-Field Hysteresis and Stability

Earlier we interpreted the decay curves (Figures 3, 4) by associating the Type I and Type II behavior with a dominant SP fraction and a stable SD fraction, respectively, in the NRM. On this interpretation, one would

explain the gradation from low-coercivity VRM to stable magnetic behavior, or from Type I to Type II behavior, by a shift in the effective domain-size distribution from the SP part towards the SD part of the spectrum. A stability criterion for testing this is the median destructive field or temperature: upon arranging the $H_{1/2}$ or $T_{1/2}$ value. This was confirmed: Table 4, combining results for all sites, shows the transition from the presence to the absence of Rayleigh loops to occur in the $H_{1/2}$ interval 110-150 oe and the $T_{1/2}$ interval 200-255°C. The only exception is Sample 15, of Type I, for which the median destructive temperature was large (415°C). The J/J_{20} - T curve of this sample (not shown) is irregular, with J/J_{20} decreasing to 0.56 at 60°C, then increasing and decreasing again at higher temperatures; it appears that, although this sample contained a VRM responsible for the Type I curve trend at low temperatures, this VRM was opposed in direction to the stable component and was insufficient in magnitude to cause, when removed, the required 50% reduction in the NRM. Except for Sample 15, the results show a qualitative association between relatively low stability and the presence of SP, and conversely, between relatively high stability and the absence of SP. A similar association was recently reported for samples of sub-aerial basalt about 70 m.y. old from west Greenland (Deutsch and Kristjansson, 1974).

Temperature Dependence of Susceptibility

Susceptibility versus temperature in the range -196°C to 650°C was measured on 13 samples. The results are of two strikingly different kinds (Figure 5a, b) and it was this difference that first led us to classify the Leg 34 basalts into two behavioral types. Sample 23 (Figure 5a)

TABLE 4
Stability of Natural Remanence Compared with the
Presence or Absence of Superparamagnetism

Heat Treatment				AF Treatment		
No.	Method	$T_{1/2}$ (°C)	Rayleigh Loop	No.	$H_{1/2}$ (oe)	Rayleigh Loop
22	C	40	Yes	14	10	Yes
44	C	90	Yes	8	20	Yes
46	C	115	Yes	4	35	Yes (c)
34	C	115	Yes (c)	39	40	Yes
9	S	135	Yes	41	45	Yes
42	S	140	Yes	45	45	Yes
17	C	175	Yes	16	60	Yes
33	S	200	Yes (c)	43	70	Yes
26	C	255	No	30	75	Yes (c)
11	C	280	No	35	75	Yes (c)
19	S	315	No	37	75	Yes (c)
15	S	415	Yes	20	85	Yes
29	S	495	No	31	110	Yes (c)
				12	150	No
				10	235	No

NOTE: No. = Samples as listed in Table 1, given here in ascending order of $T_{1/2}$ and $H_{1/2}$; C = Continuous demagnetization; S = Stepwise demagnetization; $T_{1/2}$ = Median destructive temperature, i.e., the temperature when $J/J_{20} = 0.5$; $H_{1/2}$ = Median destructive field, i.e., the field when $J/J_0 = 0.5$; Rayleigh loops were measured on untreated samples in 10 oe; (c) = Constricted Rayleigh loop.

is one of seven samples yielding Type I curves, characterized by a sharp susceptibility peak at 55°-105°C and a drop to very low k values on further heating. Moreover, in all Type I samples, k decreases continuously with decreasing temperature between that of the peak and -196°C. Susceptibility trends of this kind have been attributed (Radhakrishnamurty and Deutsch, 1974) to the presence of an SP component in the neighborhood of room temperature. In any magnetic material, it is customary to equate the temperature, T_p , of the k peak with the mean blocking temperature of the particles; then SD or MD properties occur when $T < T_p$, and SP properties when $T_c > T > T_p$, where T_c is the Curie point. As explained earlier, we attribute Type I ("SP") properties at 20°C to a range of particles straddling the SP/SD threshold. All Type I curves are moderately reversible in the range T_c to T_p and the value of T_p was always reproduced to $\leq 10^\circ\text{C}$ on cooling. However, with one exception (Sample 32), the cooling peak was found always to lie below the heating peak. These features suggest that heating to 650°C, while not destroying the SP properties of these samples, favored the formation of some SD material from SP particles, perhaps through particle growth.

Sample 6 (Figure 5b) and five other samples showed Type II behavior, with the first k peaks lying between 170° and 315°C and subsequent single or double peaks occurring in the range 450°-545°C. The first peak may be attributed (Radhakrishnamurty and Deutsch, 1974) to the presence of particles exhibiting stable SD properties at room temperature and up to T_p , while the high temperature peaks and the pronounced irreversibility of the curves may be explained by oxidation of the original SD magnetite, through heating. In Figure 5b, the susceptibility after heating is seen to decrease with falling temperature between 20°C and -196°C; this would be compatible with the carrier being SD magnetite or maghemite, to a cation-deficient (CD) phase or even maghemite, either of which should show greater coercivity at the lower temperatures. In three other Type II samples after heating the value of k was found to be greater at -196° than at 20°C, which suggests the presence of CD magnetite; cation-deficient magnetites in basalts have been reported to have smaller coercivities at -196° than at 20°C (Radhakrishnamurty et al., 1971).

Finally, MD magnetite may be diagnosed if (a) the k -T curves are more or less reversible up to T_c of magnetite (578°C), where k falls abruptly to zero; and (b) a sharp susceptibility peak occurs at the magnetite transition point (-155°C). However, no such features were found in any of our k -T curves. In SD magnetite, the transition point tends to be masked by the dominance of shape anisotropy over magnetocrystalline anisotropy.

On our interpretation one would expect that, at room temperature, samples giving Type I (SP) k -T curves will exhibit Rayleigh loops while Type II (initially SD) samples will not exhibit loops. Table 5 (second and third columns) shows that, before heating, this correlation applies without exception. Low-field hysteresis of Samples 21 and 36 (Type I), plus five samples (17, 22, 34, 44, and 46) that had shown Rayleigh loops but for which no k -T curves are available, was remeasured after

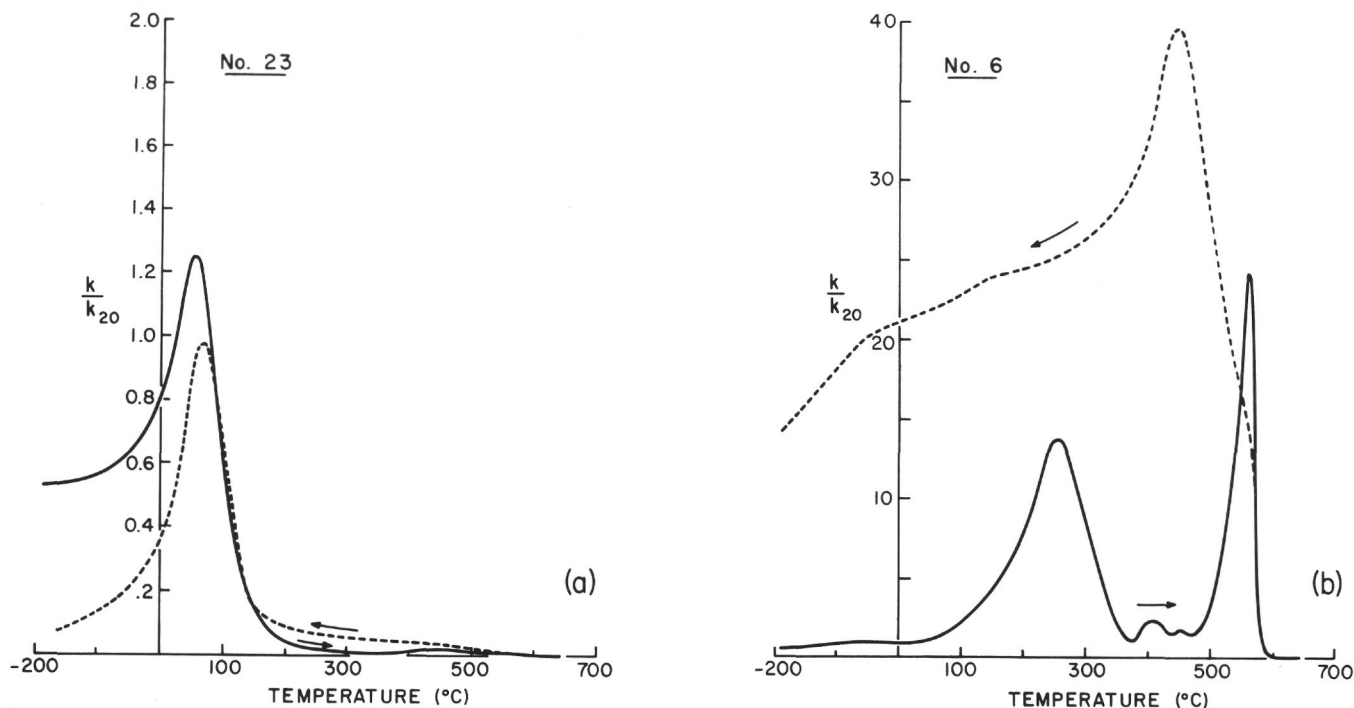


Figure 5. Normalized susceptibility-temperature (k - T) curves, heating and cooling, for (a) Type I; (b) Type II.

TABLE 5
Magnetic Properties

No.	Low-Field Loop (Rayleigh)	k - T Curves				M- T Curves			High-Field Hysteresis Loops				
		Type	Location of Peaks, T_p ($^{\circ}$ C)		T_c	$T_c - T_p$ ($^{\circ}$ C)	H_c (oe)		J_r/J_{max}		Q_n		
			Heating	Cooling			Heating	Cooling	Heating	20 $^{\circ}$ C		-196 $^{\circ}$ C	20 $^{\circ}$ C
2	no	II	170, 450/515	170	285	- , 610	115	575	115	0.6	0.3	13	
6	no	II	255, 560	460	305	- , 595	50	[515]	[240]	[0.6]	[0.7]	11	
18	yes	I	75	75	190	< 210, 590	115	690	50	0.7	0.2	2.9	
21	yes	I	70	75	160, 250	> 200, 610	90	705	50	0.7	0.2	1.0	
23	yes	I	55	65	155	< 250, 600	100	675	55	0.7	0.2	1.2	
25	yes	I	65	65	145	> 175, 550	80	695	55	0.7	0.2	2.9	
27	no	II	225, 460/525	465	345	- , 605	120					43	
28	no	II	315, 505	450/525	420	- , 555	105	[410]	[340]	[0.5]	[0.6]	19	
36	yes (c)	I	90	90	190	- , 575	100	730	85	0.7	0.3	13	
7	no	II	235, 540	505									
13	no	II	235, 515/545	480									
32	yes (c)	I	105	100									
40	yes	I	80	80									

NOTE: No. = Samples as numbered in Table 1; Low-field loop measured in 10 oe; (c) constricted Rayleigh loop; Type = See description of k - T curves. Measurements were made in the following fields: Susceptibility, k , in 0.31 oe; Magnetic moment, M , in 1,300 oe; High-field hysteresis loops in 1200 oe. $T_c - T_p$ = difference between lowest values on M- T and k - T heating curves; H_c = coercive force; J_r/J_{max} is the ratio of remanence and maximum intensity of magnetization for $H_{max} = 1200$ oe; Q_n = Koenigsberger ratio as defined in notes of Table 1. Bracketed results denote low accuracy, as the samples were weakly magnetized.

heating. Loops reappeared in all cases, except Sample 34 where a narrow constricted loop found prior to heating had now disappeared, probably due to a particle-size shift from interacting SP towards effectively SD particles upon heating. Except for this somewhat borderline case, the results show that heat treatment tends to leave the magnetic character of the Type I basalt intact. Sample 2 (k - T Type II) and two other samples (11, 26) that had not shown Rayleigh loops before heating were also remeasured after heating; as expected, no loops appeared.

Temperature Dependence of High-Field Magnetic Moment

The matching halves of the nine half samples used in k - T runs (Table 1, Set 6) were powdered for observing high-field magnetic moment versus temperature (M- T curves) with the Curie-point balance. In eight of these, high-field hysteresis had been measured before powdering (Sets 7, 7a); the ninth powder (Sample 27) was used fresh. The property observed is similar to saturation magnetization versus temperature, but it was more cor-

rect to refer to high-field M-T, rather than J_s -T, curves since the 1300-oe field used was not always sufficient for saturation.

Figure 6 shows the normalized M-T curves obtained on the same samples (23 and 6) for which k -T curves are displayed in Figure 5. The heating curve of neither sample is reproduced on cooling, but the irreversibility is more striking in the Type II case (Sample 6), in accord with the k -T results. The various Curie temperatures (T_c) for the nine samples are shown in Table 5. Since blocking temperatures in basalts usually occur within 50° to 100°C of the Curie point, one would expect the lowest T_c value in any M-T heating curve to be 50° to 100°C higher than the lowest T_p value found in the k -T heating curve for the same sample. This was approximately confirmed: Table 5 shows that, irrespective of type (I or II), the magnitude of the superparamagnetic interval $T_c - T_p$ varies from 50° to 120°C, with an average value of 100°C.

The first T_c value of all samples increased after heat treatment (Figure 6, Table 5). In Samples 18, 21, 23, and 25 (all Type I) the increase is moderate and is compatible with the transformation of some SP into SD material inferred from the k -T curves. In all Type II samples (Figure 6b, Table 5) both T_c and M increased considerably after heating and all final T_c values are close to the Curie point of magnetite. These changes are compatible with the oxidation of SD magnetite to a cation-deficient stage or maghemite, as was proposed to explain the k -T curves, and they correspond to a behavior often observed in basalts (e.g., Wilson and Smith, 1968).

We should point out that the term "Curie point" has been applied here more in a geometrical than a physical

sense, that is, T_c is specified whenever an extrapolation of the steepest part of the M-T curve crosses the temperature axis. Actually, on our interpretation, only the high T_c values on the cooling curves represent "true" Curie temperatures. All others should be considered "apparent," since the loss of ferromagnetic properties at these temperatures is attributed to thermal disordering of very small particles, rather than a loss of spontaneous magnetization as determined by mineral composition. We have found it possible to explain the thermomagnetic properties of these basalts entirely on the basis of grain-size and oxidation effects. This explanation is self-consistent, though it does not necessarily disprove the alternative explanation based on titanium content in the titanomagnetite solid-solution series. On that hypothesis all temperatures at which ferromagnetic properties vanish would be "true" Curie temperatures, and our irreversible Type II curves might be ascribed to unmixing and oxidation of an initially single-phase low-Ti titanomagnetite to magnetite and titanium minerals upon heating.

At first sight, our particle-size interpretation appears to be contradicted by the finding (Ade-Hall and Johnson, Rock Magnetism, this volume) that the basalts yielding Type I and Type II properties contain coarse-grained (15 μ to > 100 μ) and finer-grained (titano) magnetite, respectively, instead of the reverse. Against this we argue that the entire SP-SD range, and hence the inferred domain size range comprising both Type I and Type II rock, lies well below the resolving power of optical microscopes, so that it seems more relevant to consider "effective" particle sizes (corresponding to domain sizes) that are much smaller than the petrologically

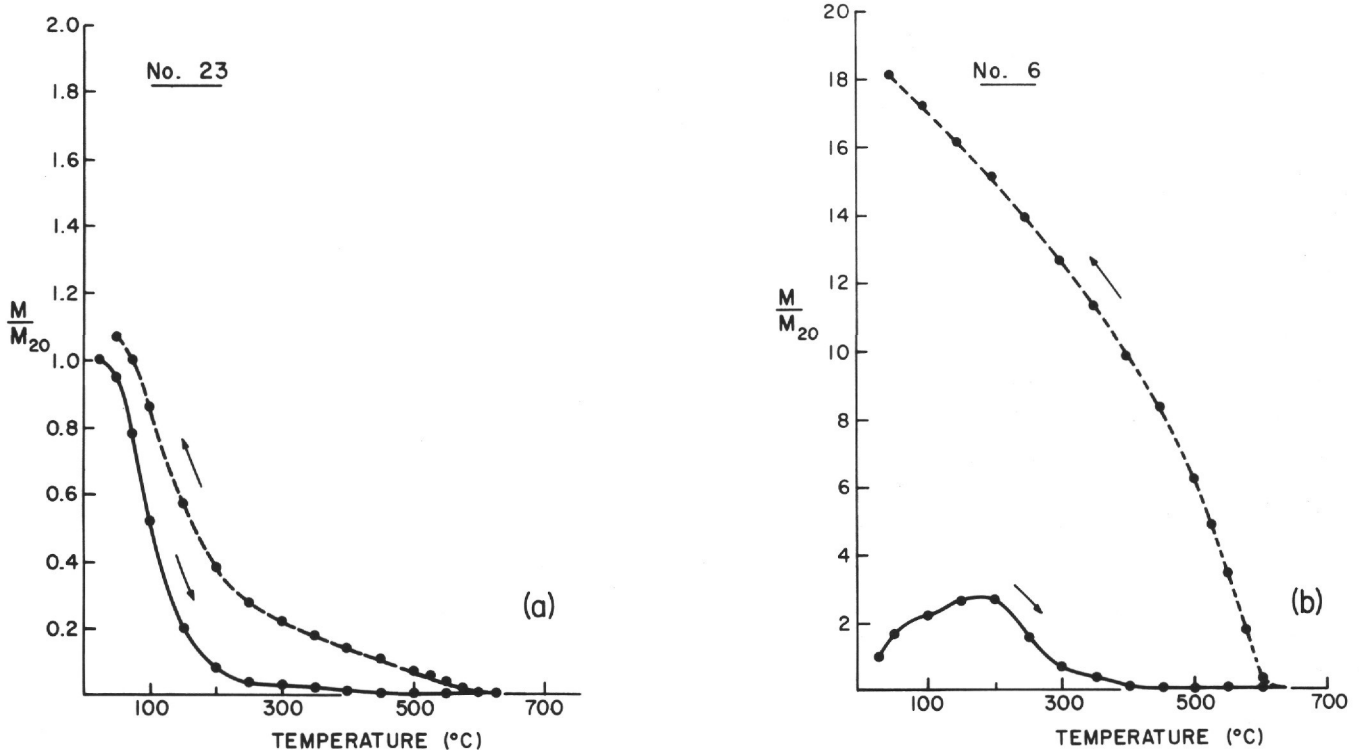


Figure 6. Normalized magnetic moment-temperature (M-T) curves, heating and cooling, for (a) Type I; (b) Type II.

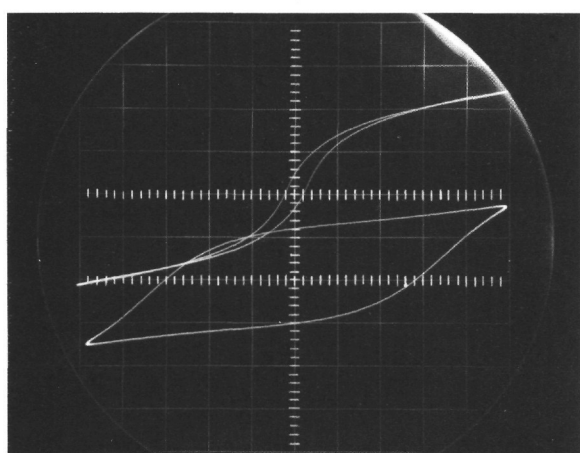
observed ones. Secondly, with a titanomagnetite model, Type I basalt corresponds to high Ti content ($x \sim 0.6$; Ade-Hall and Johnson, Review of Magnetic Properties, this volume Table 6). We would then argue that, if exsolution/oxidation were to explain the (low Ti) Type II curves, such a process should have taken place also in the Type I material, yielding irreversible curves (e.g., Ozima and Larson, 1970), whereas this interpretation is not supported by our results (Figures 5a, 6a).

Whether titanium content or magnetite grain size is primarily responsible for the observed magnetism of basalt is clearly a problem requiring much further study. In the present case, we consider the grain-size interpretation to be better supported by the results.

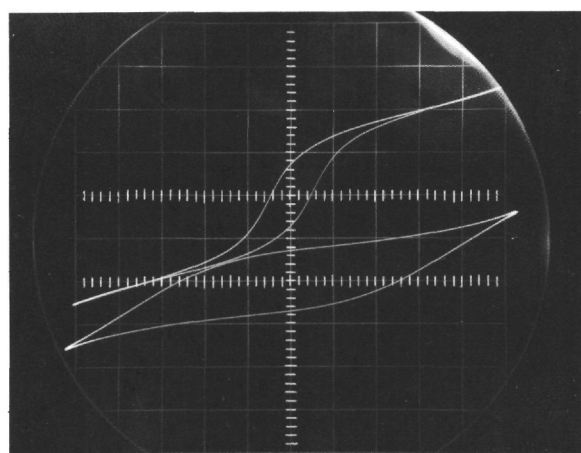
High-Field Hysteresis

Figure 7 shows hysteresis loops in fields of 1200 oe for fresh half samples of Types I and II (Figure 7a, c) and for the other halves of the same samples after k -T

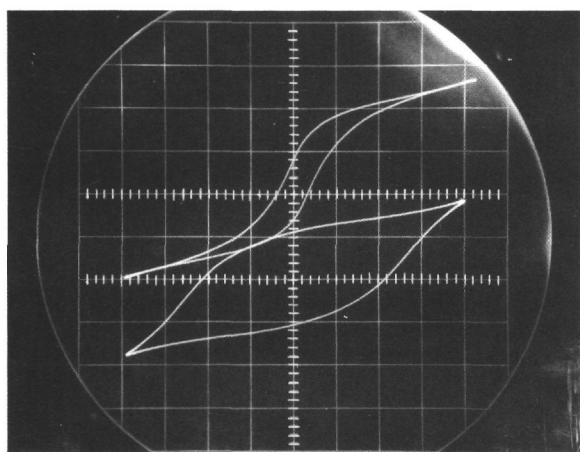
measurement (Figure 7b, d). Sample 21 of Type I (Figure 7a) has a narrow hysteresis loop at room temperature and a broad loop at -196°C . The respective coercivities are 50 and 705 oe (Table 5). Figure 7a is very similar to Figure 1 (III) in Radhakrishnamurty and Deutsch (1974), based also on basalt. This has been interpreted to reflect predominantly SP magnetite at room temperature, but which assumes a stable SD character at low temperature. At 20°C , $J_r/J_{\text{max}} = 0.2$ (Table 5), compared with the theoretical value of 0.5 expected for SD particles distributed in a nonmagnetic matrix (Stoner and Wohlfarth, 1948). Again, we attribute the fact that $J_r/J_{\text{max}} \neq 0$ either to the presence of an SD fraction (note that 20°C is less than the blocking temperature of any Type 1 sample) or to Sp interaction or both. Below -155°C , the theoretical value of J_r/J_{max} for SD magnetite is 0.8, compared with 0.7 obtained for Sample 21 at -196°C . The hysteresis parameters of four other Type I samples (Table 5, Samples 18, 23, 25, 36) are very similar



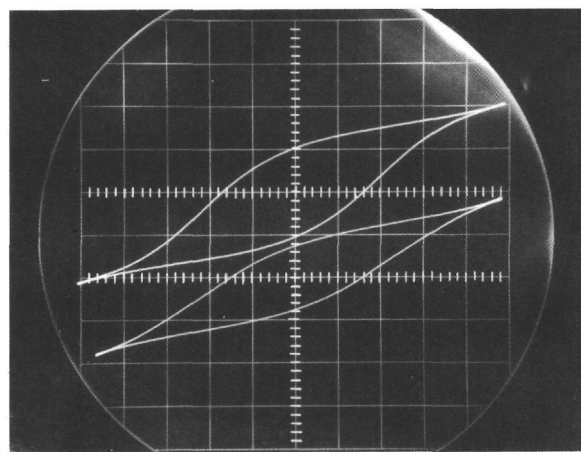
(a)



(c)



(b)



(d)

Figure 7. Photographs of hysteresis loops in 1200-oe peak on (a) a fresh sample of Type I (No. 21); (b) the same sample after heating to 650°C ; (c, d) Corresponding loops on a Type II sample (No. 2). In each pair, the lower loop was measured at -196°C and the upper loop at 20°C . Vertical scales are arbitrary.

to the above. MD magnetite appears to be ruled out, as it was also in the k - T results, because one would expect to observe very small J_r/J_{\max} values at both 20° and -196°C. Although the coercivity of MD magnetite is known to increase by a factor of two or three on cooling below the magnetite phase transition (Morrish and Watt, 1958), it would still be small at -196°C compared with H_c of SD magnetite (Radhakrishnamurty and Deutsch, 1974, fig. 1). However, Dr. D. Dunlop (personal communication) has pointed out a possible pitfall in this argument, namely that cooling through the transition to -196°C should produce an increase, not only in J_r/J_{\max} and H_c values, but also in the SD/MD or pseudo-SD/MD threshold sizes. This would mean that in our Type I samples (e.g., Figure 7a) the narrow hysteresis loops at 20°C conceivably do not represent SP (as inferred by us) but MD magnetite which changes to the stable SD structure shown by the low temperature loop. This possibility cannot be ruled out, though in view of the evidence discussed earlier we regard it as unlikely.

The heated Sample 21 (Figure 7b) has larger H_c and J_r/J_{\max} values than does the fresh sample at 20°C, though J_r/J_{\max} is still less than 0.5; again these parameters are large at -196°C. The results suggest that heating to 650°C has caused some but not all of the presumed SP component to form SD particles.

The hysteresis loops of the fresh Sample 2 of Type II are shown in Figure 7c, the distortion of the -196°C loop being due to an instrumental fault. The loops resemble those of the heated Type I samples (Figure 7b) and may be attributed to predominantly SD plus some SP component. The coercivity of the heated Sample 2 (Figure 7d) at 20°C is slightly larger than that at -196°C, while $J_r/J_{\max} = 0.5$ at both temperatures. These results suggest that the heat treatment caused oxidation of the original SD magnetite to a cation-deficient, singledomain phase (Radhakrishnamurty and Deutsch, 1974, fig. 2V). This agrees with our previous inference of CD magnetite formation from some of the k - T curves. Nine thermally demagnetized samples (Table 1, Set 3a) gave hysteresis loops similar to those either in Figure 7b or 7d, depending on whether the fresh samples had, or had not, shown Rayleigh loops.

Thus, for both Type I and Type II rocks, the high-field hysteresis results confirm our interpretation of the k - T curves. For each type, this interpretation in turn is consistent with that of the M- T and demagnetization curves and of the low-field hysteresis data.

MAGNETIC ANOMALIES

Butler (1973) has pointed out that rapid quenching of oceanic pillow basalts will cause a wide grain-size distribution of the TRM carriers, resulting in a spread of blocking temperatures located appreciably below T_c . It seems plausible that our basalts became magnetized in some such manner. This would explain the association (Table 2 and Table 5, Samples 18, 21, 23, 25) between Type I basalt and low Q_n values, at least in the samples exhibiting unconstricted Rayleigh loops. Conversely, a shift in particle-size distribution towards the SD region should have led to larger thermoremanences and smaller

susceptibilities, and hence appreciably larger Koenigsberger ratios. This appears to be confirmed by the results of a test on eight samples of Type I and four of Type II that we heated to >600°C and cooled in an 0.3-oe field to give them a TRM (Table 1, Sets 5, 3b, 6b): All 12 values of the thermoremanent Koenigsberger ratio were found to be in the range $Q_i = 16$ to 36 and the Q_i/Q_n ratios ranged from 1 to 16, with no obvious difference shown between Types I and II.

Butler (1973) further proposed from theory that SD titanomagnetite grains with initially low blocking temperatures will become superparamagnetic as they are oxidized to titanomaghemite, and his is one of several mechanisms offered to explain the large observed remanence decrease of dredged basalts with distance from the Mid-Atlantic ridge. While Butler's model is attractive in explaining SP in oceanic basalts, oxidation appears to be minor or absent in our Type I samples (see also Ade-Hall and Johnson, *Rock Magnetism*, this volume, Table 1, for low- T_c samples) and this raises a serious objection against applying his model to the Nazca plate basalts. Thus maghemitization appears to be ruled out as a cause of the SP properites found in our rocks.

Q_n values appreciably less than 10 require consideration of induced components in interpreting magnetic anomalies. Merely low Q_n , however, presents less difficulty than do large temperature gradients of k , J_n , and Q_n at the in situ temperatures of the rock. This is the case in the Leg 34 basalts, especially of Type I, as can be seen by comparing Figures 5a and 4a, Table 4 ($T_{1/2}$ values), and Table 5 (T_p values). Thus it would be misleading to use J_n and Q_n values obtained at room temperature for estimating the contribution of induced components and inferring the actual remanence of the in situ rock. Temperatures of the uppermost basalt layer are probably less than 20°C and therefore less than T_p , so that the in situ J_n and Q_n values of Type I basalt should be greater than our measured values. At greater depths, the reverse should apply. However, it is difficult to calculate reliable anomaly models from such extrapolations, since the relative distribution of Type I basalt with depth is unknown, and moreover, the susceptibility peaks of such material may occur at even lower temperatures than those we found.

The pronounced low temperature susceptibility peaks found in all Type I samples (e.g., Figure 5a) are analogous to the classical Hopkinson peak (Hopkinson, 1889) often seen just below the true Curie point of ferromagnetics; e.g., the high temperature maxima in Figure 5b appear to be Hopkinson peaks. Dunlop (1974) has made the interesting suggestion that the relatively large magnetizations sometimes required for interpreting deep-seated anomalies, which must be of induced origin, can be explained by thermal enhancement of susceptibility due to the Hopkinson effect near the Curie point isotherm. Although any rocks having large Hopkinson peaks near the magnetite Curie point (578°C) are probably too deep seated to have much effect on the observed anomalies over the Nazca plate drilling sites, the low-temperature peaks described by us here evidently constitute a highly relevant application of Dunlop's mechanism.

ACKNOWLEDGMENTS

We are grateful to Dr. C. Radhakrishnamurty (Bombay) for thorough discussions and to Dr. David Dunlop (Toronto) for a critical review that led to several improvements in the manuscript. We also appreciate assistance in measurements from Philip Kirby (Memorial University of Newfoundland). This research was supported by Operating Grant A-1946 from the National Research Council of Canada.

REFERENCES

- Bean, C.P. and Livingston, J.D., 1959. Superparamagnetism: *J. Appl. Phys.*, v. 30, p. 120S-129S.
- Butler, R.F., 1973. Stable single-domain to superparamagnetic transition during low-temperature oxidation of oceanic basalts: *J. Geophys. Res.*, v. 78, p. 6868-6876.
- Christie, K.W. and Symons, D.T.A., 1969. Apparatus for measuring magnetic susceptibility and its anisotropy: *Geol. Surv. Canada Paper* 69-14.
- Deutsch, E.R. and Kristjansson, L.G., 1974. Paleomagnetism of Late Cretaceous-Tertiary volcanics from Disko Island, West Greenland: *Geophys. J.*, v. 39, p. 343-360.
- Deutsch, E.R., Kristjansson, L.G., and May, B.T., 1971. Remanent magnetism of Lower Tertiary Lavas on Baffin Island: *Canadian J. Earth Sci.*, v. 8, p. 1542-1552.
- Dunlop, D.J., 1965. Grain distribution in rocks containing single domain grains: *J. Geomag. Geoelectr.*, v. 17, p. 459-471.
- , 1974. Thermal enhancement of magnetic susceptibility: *J. Geophys./Zeits. Geophys.*, v. 40, p. 439-451.
- Herron, E.M., 1972. Sea-floor spreading and the Cenozoic history of the east-central Pacific: *Geol. Soc. Am. Bull.*, v. 83, p. 1671-1692.
- Hopkinson, J., 1889. Magnetic and other physical properties of iron at a high temperature: *Phil. Trans. Roy. Soc. London, Ser. A*, v. 180, p. 443.
- Hart, S.R., et al., 1974. Deep-sea drilling project: Leg 34: *Geotimes*, v. 19, p. 20-24.
- Likhite, S.D., Radhakrishnamurty, C., and Sahasrabudhe, P.W., 1965. Alternating current electromagnetic type hysteresis loop tracer for minerals and rocks: *Rev. Sci. Instr.*, v. 36, p. 1558-1560.
- Lowrie, W., 1974. Oceanic basalt magnetic properties and the Vine and Matthews hypothesis: *J. Geophys./Zeits. Geophys.*, v. 40, p. 513-536.
- Lowrie, W. and Fuller, M., 1971. On the alternating field demagnetization characteristics of multidomain thermoremanent magnetization in magnetite: *J. Geophys. Res.*, v. 76, p. 6339-6349.
- Morrish, A.H. and Watt, L.A.K., 1958. Coercive force of iron oxide micropowders at low temperatures: *J. Appl. Phys.*, v. 29, p. 1029-1033.
- Neel, L., 1970. Interpretation des cycles d'hystérésis entranglés de certaines basaltes: *C. R. Acad. Sci. Paris*, v. 270, p. 1125-1130.
- Ozima, M. and Larson, E.E., 1970. Low- and high-temperature oxidation of titanomagnetite in relation to irreversible changes in the magnetic properties of submarine basalts: *J. Geophys. Res.*, v. 75, p. 1003-1017.
- Pätzold, R., 1972. High-temperature magnetic susceptibility bridge: Unpublished M.Sc. thesis, Memorial University of Newfoundland.
- Radhakrishnamurty, C. and Deutsch, E.R., 1974. Magnetic techniques for ascertaining the nature of iron grains in basalts: *J. Geophys./Zeits. Geophys.*, v. 40, p. 453-456.
- Radhakrishnamurty, C. and Likhite, S.D., 1970. Relation between thermal variation of low field susceptibility and magnetic hysteresis in basalts: *Earth Planet. Sci. Lett.*, v. 9, p. 294-298.
- Radhakrishnamurty, C. and Sastry, N.P., 1970. A single-domain grain model for the low field constricted hysteresis loops of some basalts: *Proc. Indian Acad. Sci.*, v. 72, p. 94-102.
- Radhakrishnamurty, C., Likhite, S.D., Raja, P.K.S., and Sahasrabudhe, P.W., 1971. Magnetic grains in Bombay columnar basalts: *Nature, Phys. Sci.*, v. 235, p. 33-35.
- Stoner, E.C. and Wohlfarth, E.P., 1948. A mechanism of magnetic hysteresis in heterogeneous alloys: *Phil. Trans. Roy. Soc. London, Ser. A*, v. 240, p. 599-642.
- Wilson, R.L., 1962. An instrument for measuring vector magnetization at high temperatures: *Geophys. J.*, v. 7, p. 125-130.
- Wilson, R.L. and Smith, P.J., 1968. The nature of secondary natural magnetizations in some igneous and baked rocks. *J. Geomag. Geoelectr.*, v. 20, p. 367-380.